

Novel Calcium Potentiometric Selective Electrode Based on Lisinopril Functionalized Multi-walled Carbon Nanotubes-NiO Nanocomposite

Nehad A. Abdallah^{1,2}

¹ Pharmacognosy and Pharmaceutical Chemistry Department, College of Pharmacy, Taibah University, Al-Madinah Al-Mounawarah 30078, KSA

² Experiments and Advanced Pharmaceutical Research Unit, Faculty of Pharmacy, Ain Shams University, Cairo 1156, Egypt.

*E-mail: nehad.amin@gmail.com

Received: 25 March 2021 / Accepted: 12 May 2021 / Published: 30 June 2021

A novel carbon paste electrode utilizing a lisinopril molecule as a recognition element for the selective determination of free Ca^{2+} ions was developed. The fabrication of the sensor was established by the covalent attachment of lisinopril to the surface of the MWCNTs-NiO nanocomposite. The formed composite was characterized by FT-IR, TEM, and XRD. This unique design has led to high selectivity and stability of the studied carbon paste electrode. It revealed a Nernstian slope of 30.4 ± 0.52 mV/decade with wide linearity ranging from 1×10^{-2} mol L⁻¹ to 1×10^{-8} mol L⁻¹. The electrode showed high sensitivity to Ca^{2+} ion. The LOD was found to be 3.5×10^{-9} mol L⁻¹. The proposed sensor was successfully applied for the determination of Ca^{2+} concentration in various media such as pharmaceutical tablets, tap water, soil drainage water samples and human serum samples. The resulted recovery of the sensor was in the range of 94.2% - 102.1% with acceptable precision and reproducibility.

Keywords: Calcium; Carbon paste electrode; potentiometry; MWCNTs; NiO nanoparticles; Lisinopril

1. INTRODUCTION

Lisinopril (Lis) is (2S)-1-[(2S)-6-amino-2-[[[(2S)-1-hydroxy-1-oxo-4-phenylbutan-2-yl] amino] hexanoyl] pyrrolidine-2-carboxylic acid, Fig. 1. It is an angiotensin-converting enzyme (ACE) inhibitor that is used for the treatment of hypertension and congestive heart failure [1]. Chemically, the lisinopril molecule has two carboxyl groups; prolyl COOH and central COOH that are dissociated at pH above 5. This allows lisinopril to interact easily with metal ions, making it a good chelating agent. Lisinopril coordinates to the metal ions as either monodentate or bidentate ligand or forms various coordinating

Calcium is considered an important element in the formation of bones and teeth. The calcium ion is also important for the heart, the nerves, and blood-clotting systems. Several analytical methods were applied for the quantitation of the Ca^{2+} ion concentration such as spectrophotometry [14-16], spectrofluorimetry [17-19], HPLC [20-24], capillary electrophoresis [25-27], voltammetry [28-30], and potentiometry [31-39]. All of the stated potentiometric sensors depend on the development of ion-selective PVC-based electrodes with the incorporation of different calcium ionophores. As far as we know, no solid-contact carbon paste electrode with the support of MWCNTs was designed in the potentiometric determination of Ca^{2+} ion. The reported potentiometric CPE was based on the mixing of the graphite powder with a synthesized ionophore in the presence of acetophenone without the incorporation of MWCNTs as a conducting layer [39].

Our study aims to develop a new sensitive CPE for the determination of Ca^{2+} ion by taking the advantage of the chelating nature of the lisinopril molecule to be utilized as a recognition element for the first time. The electrode paste was composed of MWCNTs that were decorated with Nickel oxide (NiO) nanoparticles as a transducer element. This was followed by the covalent attachment of lisinopril to the surface of MWCNTs-NiO through carboxylation of the surface of NiO nanoparticles followed by amidation reaction with the lisinopril amino group with the aid of thionyl chloride in dimethylformamide medium. The proposed sensor was successfully used for the quantitation of Ca^{2+} ion in tablets, tap water, soil drainage water and human serum samples. It was also effectively applied in the in-line monitoring of the dissolution profile of calcium tablets without the need for frequent sampling at every time interval.

2. PROCEDURE

2.1. Reagents and chemicals

The chemicals in this study were of analytical grade. Graphite powder, MWCNTs (> 90%, diameter 50-90 nm), Lisinopril (Lis) standard, and Nickel oxide (NiO) nanoparticles (> 95%, diameter < 50 nm) were purchased from Sigma Aldrich, Germany. Potassium tetrakis [p-chlorophenylborate] (KTPCIPB) was obtained from Acros-Organics, USA. TMSEDTA (N-trimethoxysilylpropyl ethylene diamine triacetic acid), TEOS (tetra-ethyl-ortho-silicate) were from Sigma-Aldrich. Tetrahydrofuran (THF) and N, N dimethylformamide (DMF) were purchased from Fluka, USA. Calcium chloride standard powder, H_2SO_4 and HNO_3 were obtained from Sigma Aldrich.

2.2. Instruments

Jenway digital ion analyzer pH 3510 (UK) was connected to the indicator electrode and Thermo-Orion double junction Ag/AgCl (900201) as the external reference electrode for potentiometric measurement. Samples were measured under continuous stirring using JLab-Tech magnetic stirrer, LMS-1003.

2.3. Standard solutions

A calcium ion stock solution of 1×10^{-1} mol L⁻¹ was prepared by weighing the appropriate amount of the standard CaCl₂ powder in a 50 mL volumetric flask using deionized water as a solvent. Working standard solutions of concentrations ranged from 1×10^{-2} mol L⁻¹ to 1×10^{-10} mol L⁻¹ were prepared by diluting the relative stock solution with deionized water.

2.4. Carbon paste electrode fabrication procedure

2.4.1. Purification of MWCNTs and decoration with NiO nanoparticles:

As reported in our previous work [8], purification and functionalization of the crude MWCNTs with the carboxylic groups to increase the dispersibility and stability was performed by its treatment in 500 mL of a mixture of H₂SO₄ and HNO₃ in the ratio (3: 1 v/v) with ultrasonication for 2 h. The solution was refluxed for 2 h to minimize the tube damage. Then, the solution was cooled, filtered and washed with deionized water until the filtrate became neutral. The washed nanotubes were dried under vacuum at 70 °C for 8 h. By the application of the oxidation process, carboxylic, carbonyl and hydroxyl groups were presented on the nanotubes surfaces as they were required to anchor the guest species of the metal oxide nanoparticles to the CNTs. Approximately 0.5 g of the acid-treated MWCNTs was mixed with nearly 0.5 g of NiO nanoparticles after the addition of 500 mL of DMF. The components were allowed to dissolve by ultra-sonication for 48 h at room temperature which subsequently resulted in a solution of MWCNTs-NiO nanohybrid that was dried at 25 °C overnight to evaporate the solvent.

2.4.2. Grafting of Lisinopril on the surface of MWCNTs-NiO nanocomposite

The grafting process was based on the covalent attachment of carboxylated MWCNTs-NiO nanocomposite to the lisinopril molecule through the formation of an amide bond. About 10 mL of the concentrated ammonia was added to 80% ethanoic suspension of MWCNT-NiO nanocomposite under continuous sonication at room temperature and followed by the dropwise addition of 5 mL of TEOS. The product of MWCNTs-NiO-SiO₂ was rinsed with deionized water and vacuum dried. Then 0.5 g of MWCNT-NiO-SiO₂ nanocomposite was dispersed in 30 mL of toluene and refluxed for 10 h at 70 °C after the addition of 1 g of TMS-EDTA. Filtration of the produced MWCNTs-NiO-COOH was done and followed by rinsing with ethanol and vacuum drying at 70 °C. About 40 mL of thionyl chloride was added to a dispersion of MWCNTs-NiO-COOH in the DMF medium and refluxed for 12 h at 70 °C. Filtration of the produced substance was done and followed by washing with anhydrous THF and diethyl ether, and vacuum drying at 60 °C. 0.1 g of lisinopril dihydrate was added to the produced MWCNTs-NiO-COCl in the DMF medium and ultra-sonicated for 1 h and then refluxed for 12 h at 70 °C. The formed MWCNTs-NiO-Lis solid composite was collected by filtration, washing with THF, and then vacuum drying at 60 °C.

2.4.3. Preparation of the CPE

The proposed electrode was fabricated by homogenous mixing of 30 mg of graphite powder with 40 mg of paraffin oil, 10.0 mg of (KTPCIPB), and 30 mg of MWCNTs-NiO-Lis composite for 30 min in a glass mortar. The Teflon cavity of the electrode was tightly packed with the carbon paste. A new surface was obtained by pushing the electrode steel screw which was smoothed by using a clean filter paper.

2.5. Potentiometric measurement

The *e.m.f.* measurements were recorded at ambient temperature with the following electrochemical cell: Ag /AgCl double junction reference electrode/ sample test solution/ Lis covalently attached to MWCNTs-NiO oil paste/ copper wire. The reference and indicator electrodes were dipped in 25 mL of the solution with magnetic stirring at a constant rate. Deionized water was used for washing the studied electrode between measurements.

3. RESULTS AND DISCUSSION

3.1. Characterization of the prepared MWCNTs-NiO-Lis nanocomposite

3.1.1. FT-IR spectroscopic characterization

The acid-treated MWCNTs spectrum, Fig.2 (a), demonstrated some characteristic bands which are positioned at 1725 cm^{-1} , 1577 cm^{-1} and 1375 cm^{-1} that are associated with C=O stretching of the carboxylic group, C=C stretching of the intrinsic arrangement of CNTs, and O-H bending vibration, respectively. The OH stretching vibration is represented with a major band positioned at 3467 cm^{-1} . The bands extended from 2846 cm^{-1} to 2940 cm^{-1} are associated with the stretching of the C-H bond. The reported bands confirmed the efficient introduction of the carboxyl groups onto the surface of MWCNTs after acid treatment. The MWCNTs-NiO nanocomposite spectrum in Fig. 2(b) showed different bands of low intensities at 3440 cm^{-1} and 1712 cm^{-1} due to the anchoring of NiO nanoparticles to MWCNTs using the carboxyl groups on their surfaces. Two absorption bands at 565 cm^{-1} and 1105 cm^{-1} are monitored. They are related to Ni-O stretching. Ni-O-Ni stretching is represented as another band at 1402 cm^{-1} . The MWCNTs-NiO-Lis composite spectrum in Fig. 2(c) displayed an absorption band at 1024 cm^{-1} of Si-O-Si stretching vibration that confirmed the silanization of the surface of the NiO nanoparticles. Different bands extended from 3300 cm^{-1} to 3560 cm^{-1} are corresponding to the N-H stretching of the amide link and O-H stretching of the Lisinopril free carboxyl groups. The amide link formation can be confirmed by the stretching vibration of the C-N of the amide link at 1253 cm^{-1} and by the bending vibrations (scissoring & wagging) of N-H at 1617 cm^{-1} and 754 cm^{-1} .

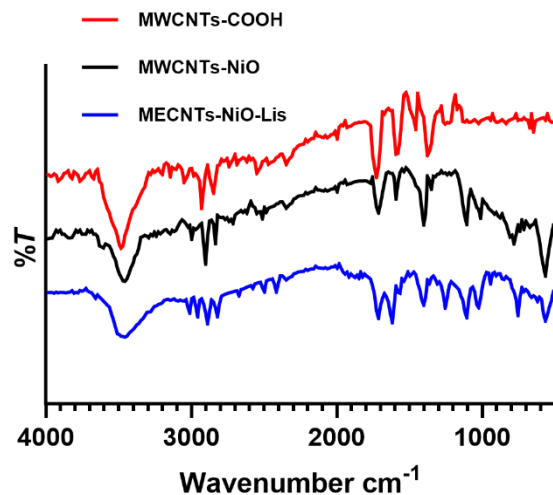


Figure 2. FT-IR analysis of (a) MWCNTs-COOH, (b) MWCNTs-NiO nanocomposite, and (c) MWCNTs-NiO-Lis composite.

3.1.2. XRD

The MWCNTs XRD, Fig. 3(a) displayed a sharp prominent peak at 2θ of 25.9° that is related to the carbon skeleton of the MWCNTs sheets. The MWCNTs-NiO nanocomposite XRD, Fig. 3(b), was described by significant peaks at 2θ of 37.2° , 43.3° , 62.6° , 75.4° , and 79.3° that are associated with the crystal structure of NiO nanoparticles. It also showed a diffraction peak at 26.0° of the MWCNTs. These results prove that the MWCNTs have not been destroyed after the acid treatment and successfully loaded with NiO nanoparticles on its surface. In the XRD of MWCNTs-NiO-Lis composite Fig. 3(c), overlapping of the strong peak of MWCNTs at 25.9° with that of lisinopril was observed. Also, the presence of low-intensity peaks in the range of 2θ of 7° to 30° indicated the change of the structure of MWCNTs-NiO composite due to the covalent attachment to the Lisinopril molecule. It is noticed that the peaks of NiO nanoparticles are of low intensity. These data indicate that the composite is formed of three phases which are the NiO nanoparticles and the lisinopril that are effectively deposited and functionalized over the MWCNTs surface. The diffraction peaks of each of the acid-treated MWCNTs, NiO nanoparticles, and lisinopril are in good agreement with the reported values in the literature [8, 40-42].

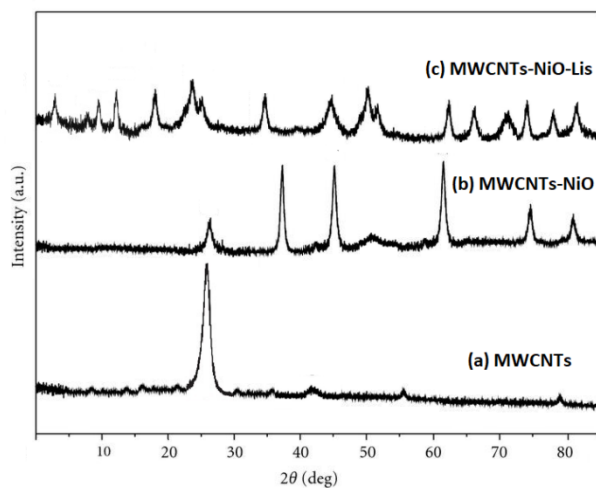


Figure 3. XRD pattern of (a) MWCNTs-COOH (b) MWCNTs-NiO nanocomposite and (C) MWCNTs-NiO-Lis composite.

3.1.3. TEM

The surface morphology changes were studied with the aid of TEM. The acid-treated MWCNTs, Fig. 4(a), appeared as tubular structures with smooth surfaces with an outer diameter of about 50-90 nm and almost all the end caps were revealed. When the NiO nanoparticles decorated the surfaces of MWCNTs, Fig. 4(b), the TEM image showed the formation of homogeneously spread clusters of the NiO around the nanotubes which can be attributed to the strong ionic interaction between them. The thickness of the CNTs was varied from 70 nm to 100 nm. The TEM image of the MWCNTs-NiO-Lis composite, Fig. 4(c), showed an increase in the size of the MWCNTs coated particles and became with an average thickness of 130-180 nm.

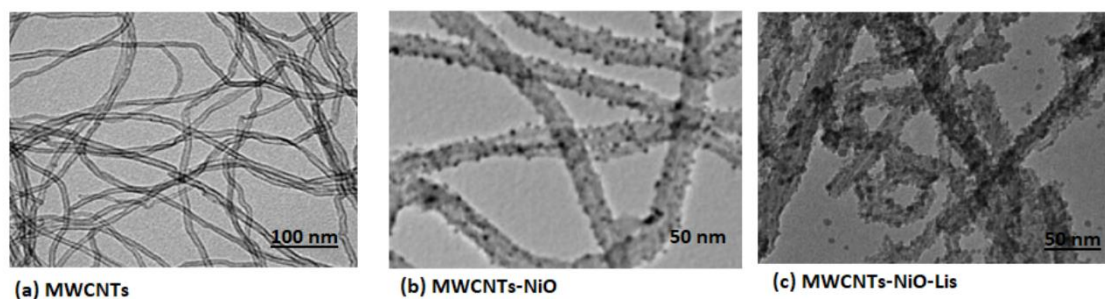


Figure 4. TEM images of (a) MWCNTs-COOH (b) MWCNTs-NiO nanocomposite and (C) MWCNTs-NiO-Lis composite.

3.2. Optimization of the CPE composition

Generally, the solid contact CPE is composed of a recognition element that defines the selectivity of the membrane, and a transducer that translates the recognition event into a measurable signal with

high sensitivity. In this study, lisinopril was applied as a recognition element. It acts as a ligand that forms a coordination complex with the metal ions via the two carboxyl groups (prolyl COOH and central COOH) [43, 44]. MWCNTs decorated with NiO nanoparticles were applied as an effective transducer material. As summarized in Table 1, Different sensors with different paste compositions were fabricated to optimize the response characteristics. The bare sensor was fabricated by mixing the graphite powder and the paraffin oil homogenously in a ratio of (60: 40% w/w) and producing consistent, and mechanically robust carbon paste. The non-covalent functionalization of the lisinopril to the MWCNTs-NiO composite was prepared by their simple mixing together (sensor 5). It depends on the weak ionic interaction between the nanocomposite and the lisinopril. It showed a long response time (> 1 min) and a non-ideal Nernstian slope for divalent cation with a limited linearity range. This could be explained by the frequent leaching of the recognition element (lisinopril) from the paste to the aqueous phase due to its inherent hydrophilicity that affects the electrode response to Ca^{2+} ions. The covalent attachment of the lisinopril to the surface of MWCNTs-NiO nanocomposite was performed through an amidation reaction using thionyl chloride without altering the inner structure of the nanotubes as well as their ionic structure (sensors 6-11). Due to the chelating properties of lisinopril to Ca^{2+} ions, the selectivity of the sensor was improved. Different electrodes with different compositions were designed. The contribution of NiO nanoparticles was studied by recording the response characteristics of sensors 3 and 4. It was proved that the presence of metal oxide nanoparticles positively influences electrode performance. NiO nanoparticles enhance the sensitivity, response time and Nernstian slope of the sensor.

Table 1. Optimization of the CPE composition

	Graphite (mg)	MWCNTs (mg)	MWCNTs-NiO (mg)	MWCNTs-NiO-Lis (mg)	KTpCIPB (mg)	Lis. (mg)	Paraffin Oil (mg)	Linearity range (mol L ⁻¹)	LOD (mol L ⁻¹)	Slope (mV/decade)	Response time (s)
1	60	-	-	-	-	-	40	$2 \times 10^{-3} - 1 \times 10^{-2}$	1×10^{-4}	18.7 ± 0.31	45
2	40	-	20	-	-	-	40	$1 \times 10^{-4} - 5 \times 10^{-2}$	3.5×10^{-5}	21.6 ± 0.36	30
3	30	30	-	-	-	-	40	$1 \times 10^{-3} - 5 \times 10^{-1}$	1×10^{-4}	19.7 ± 0.28	40
4	30	-	30	-	-	-	40	$5 \times 10^{-5} - 1 \times 10^{-2}$	3.5×10^{-6}	23.5 ± 0.45	30
5	30	-	20	-	10	10	40	$1 \times 10^{-5} - 1 \times 10^{-3}$	8.5×10^{-6}	24.9 ± 0.38	40
6	30	-	-	30	-	-	40	$1 \times 10^{-6} - 1 \times 10^{-3}$	4.0×10^{-7}	24.7 ± 0.29	20
7	25	-	-	35	-	-	40	$2 \times 10^{-6} - 4 \times 10^{-3}$	1.7×10^{-7}	26.4 ± 0.63	20
8	30	-	-	30	10	-	40	$1 \times 10^{-8} - 1 \times 10^{-2}$	3.5×10^{-9}	30.4 ± 0.52	10
9	40	-	-	20	10	-	40	$2 \times 10^{-7} - 5 \times 10^{-3}$	6.2×10^{-8}	28.5 ± 0.58	10
10	20	-	-	40	10	-	40	$6 \times 10^{-7} - 6 \times 10^{-3}$	7.2×10^{-8}	29.2 ± 0.67	10
11	30	-	-	30	5	-	40	$2 \times 10^{-7} - 4 \times 10^{-3}$	5.9×10^{-8}	29.1 ± 0.82	15

Results in Table 1 revealed the change in the electrode response characteristics with the application of either MWCNTs-NiO (sensors 2, 4) or MWCNTs-NiO-Lis (sensors 6-11) composites. The introduction of the lisinopril molecules improves the response characteristics by easing the accessibility of Ca^{2+} ions to the electrode through the formation of coordination complex by the reaction with its free carboxyl groups. The phase boundary potential is generated as a result of the formation of such a coordination complex. The addition of KTpCIPB as a cation exchanger supports the complexation of the lisinopril and Ca^{2+} ions by providing lipophilic ionic sites in the paste matrix. It helps to attain the

potentiometric equilibrium rapidly and to create the phase-boundary potential. The optimum composition of the studied sensor was represented as sensor 7.

3.3. Performance characteristics of the CPE (Linearity, response time, precision, and stability)

IUPAC guidelines [45] were applied to study the potentiometric behavior of the proposed CPE. The response characteristics of the studied electrode were summarized in Table 2. The CPE showed a linear response ranged from 1×10^{-2} mol L⁻¹ to 1×10^{-8} mol L⁻¹ with a Nernstian slope of 30.4 ± 0.52 mV/decade, which is characteristic of the divalent cation (30 mV/decade). Fig. 5 represents the dynamic time trace of the response of the proposed sensor over the calcium concentration range from 1×10^{-1} mol L⁻¹ to 1×10^{-10} mol L⁻¹. The LOD was found to be 3.5×10^{-9} mol L⁻¹. It was calculated with the aid of the linear calibration curve slope using the equation of $LOD = 3 S / b$, where S is the standard deviation of the y-axis of 5 replicates of the blank and b is the slope of the linear calibration curve. The repeatability $RSD\%$ was calculated after five successive measurements of each of three calibrators (1×10^{-2} - 1×10^{-5} - 1×10^{-8} mol L⁻¹) of Ca²⁺ ions standard solution within a day. The intermediate precision $RSD\%$ was calculated after five measurements of the three calibrators in ten consecutive days. Six independently synthesized sensors were fabricated to study the sensor reproducibility. The $RSD\%$ was calculated for five replicates of each of the three standard concentrations of Ca²⁺ ions and represented in Table 2.

Table 2. The electrochemical characteristics of the proposed sensor

Parameter	CPE response
Concentration range (mol L ⁻¹)	$1 \times 10^{-2} - 1 \times 10^{-8}$
Slope (mV/decade)	30.4 ± 0.52
Intercept	434.19
Correlation coefficient	0.998
LOD (mol L ⁻¹)	3.5×10^{-9}
Response time (s)	10 ± 0.2
Stability (days)	106
Working pH range	6 - 11
Average recovery ¹	99.5 ± 1.13
Intraday precision ² ($RSD\%$)	0.97
Interday precision ² ($RSD\%$)	1.45
Reproducibility ³ ($RSD\%$)	1.67

¹ Average of five determinations of seven concentration levels.

² Average of five determinations of three concentration levels (1×10^{-2} - 1×10^{-5} - 1×10^{-8} mol L⁻¹).

³ Average of five determinations of three concentration levels (1×10^{-2} - 1×10^{-5} - 1×10^{-8} mol L⁻¹) using six independently fabricated sensors.

The obtained intraday and interday $RSD\%$ values were calculated to be 0.97% and 1.45%, respectively. These values indicated the reproducibility and the precision of the proposed sensor. The

electrode was characterized by rapid response (< 12 s) and a stable potential over the linear concentration range. The electrode reversibility was studied and approved by measuring its response in an ascending and descending order relative to the concentration range as shown in Fig. 6. The CPE lifetime was evaluated by constructing the calibration plot and testing its characteristics on different days under normally applied conditions. During this time the slope did not fluctuate by more than ± 2 mV/decade and no variation in the potential recorded (not more than ± 3) over 106 days for the same carbon paste surface without any renewal action. After this period of dry storage, a remarkable decrease in the calibration slope was observed. The renewed surface presented accurate and reliable data. The lifetime of the studied sensor could be prolonged to nearly 12 months by surface renewal every 106 days for 3 - 4 times. The prolonged life of the electrode is likely attributed to the un-leaching of the recognition element from the electrode matrix due to its covalent attachment to the transducer layer. Therefore, the proposed CPE can be stored in dry conditions for prolonged periods with no significant loss of performance characteristics.

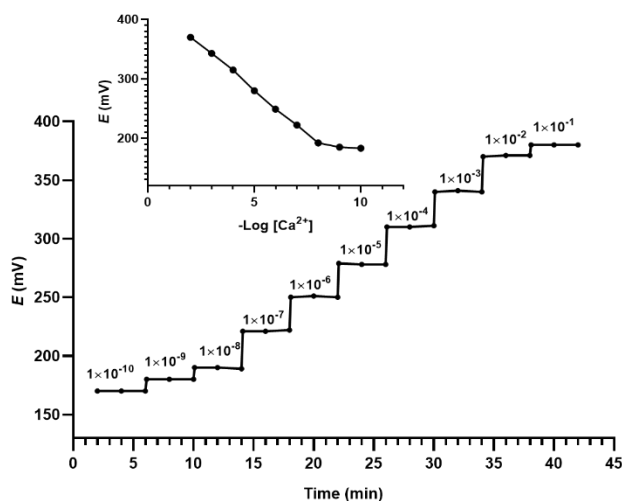


Figure 5. The time trace of the response of the proposed CPE over the concentration range from 1×10^{-2} mol L⁻¹ to 1×10^{-10} mol L⁻¹.

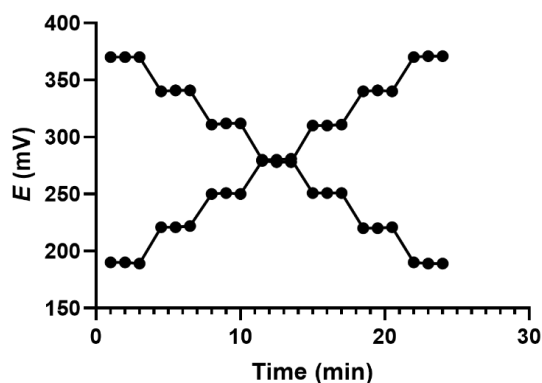


Figure 6. The dynamic response time of the proposed CPE from low to high and high to low concentrations.

3.4. Influence of pH

The influence of the pH on the response of the studied electrode was studied. Two standard Ca^{2+} ion solutions at different pH values were prepared using 40 mM of Britton-Robinson buffer solution with pH ranging from 2 to 12. The buffer solutions were prepared by mixing 40 mM of all necessary components (phosphoric acid, acetic acid and boric acid) and adjusting the pH with 0.2 M sodium hydroxide. It indicated that the electrode potential values were stable within the pH range from 6.0 to 11.0 as represented in Fig. 7. It might be explained by the presence of the free calcium ions that can interact easily with the ionized carboxylic groups of the ligand lisinopril ion at this pH. Increasing the sensor response below pH 6 may be related to the high concentration of the hydronium ion which competes with the Ca^{2+} ion causing protonation of lisinopril in the membrane matrix. The reduction in the electrode potential above pH 11 could be explained by the formation of calcium hydroxyl in the solution. Therefore, pH 7 was chosen as an optimum pH in the sample determination.

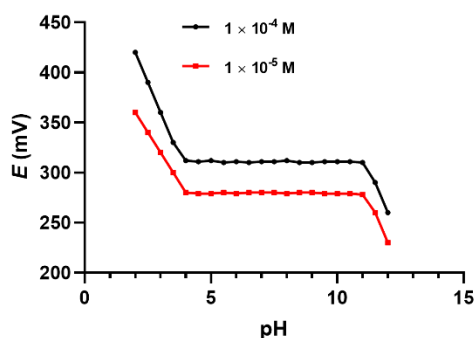


Figure 7. Effect of pH on the potentiometric response of the proposed CPE using 1×10^{-4} mol L^{-1} and 1×10^{-5} mol L^{-1} Ca^{2+} standard solutions.

3.5. Selectivity and comparison with the literature's potentiometric electrodes

The response of the proposed sensor to the Ca^{2+} ion (target analyte) compared to other interfering ions is termed selectivity and is expressed by the selectivity coefficient $K_{A,B}^{\text{pot}}$. The selectivity coefficient was evaluated by the separate solution method using 1×10^{-4} mol L^{-1} Ca^{2+} ion standard solution and 1×10^{-4} mol L^{-1} interfering ion solution. The $K_{A,B}^{\text{pot}}$ was calculated by the Nicolsky-Eisenman equation [45]:

$$\log K_{A,B}^{\text{pot}} = \frac{(E_B - E_A)Z_A F}{(2.303 RT)} + \left(1 - \frac{Z_A}{Z_B}\right) \text{Log} [A]$$

Where Z_A and Z_B are the charges of the analyte ion and the interfering ion, respectively. The calculated $K_{A,B}^{\text{pot}}$ values are shown in Table 3. They proved an outstanding selectivity of the studied electrode for Ca^{2+} ions with no substantial effect from other cationic species.

Table 3. Potentiometric selectivity coefficient ($\log K_{Ca^{2+}, Interferent}^{pot}$) for the proposed CPE

Interfering ions	($\log K_{Ca^{2+}, Interferent}^{pot}$)
Mg ²⁺	-3.08
Mn ²⁺	-3.12
Cu ²⁺	-4.88
Al ³⁺	-4.78
Pb ²⁺	-3.23
Na ⁺	-4.79
Hg ²⁺	-4.82
Co ²⁺	-3.07
Sr ²⁺	-3.73
Ba ²⁺	-4.66
Fe ²⁺	-2.86

Depending on the literature survey, some potentiometric sensors were designed for the estimation of Ca²⁺ ions in different samples. As we mentioned in the introduction section, the reported calcium ions sensors were based on the application of PVC-membranes with the aid of different calcium ionophores. The reported CPE was based on the mixing of the graphite powder with a synthesized ionophore in the presence of acetophenone [39]. The concept of the covalent attachment of the recognition element to the surface of the MWCNTs- Metal oxide composite has been recently used for the fabrication of different CPEs for the determination of different analytes [8, 47, and 48]. However, the application of the lisinopril molecule as a recognition element was utilized for the first time in this work. The potentiometric response characteristics of the studied CPE were compared with the other reported ones and summarized in Table 4. The results showed that the proposed sensor displayed better response time, sensitivity, slope, lifetime, and wider linearity range.

Table 4. Comparison of the potentiometric response characteristics of the proposed Ca²⁺ sensor with the literature ones.

Electrode	Linearity range (mol L ⁻¹)	LOD (mol L ⁻¹)	Slope (mV/decade)	Response time (s)	Lifetime	pH range	Ref
PVC+ NPOE + calcium ionophore II	2×10 ⁻⁵ – 3×10 ⁻⁴	6×10 ⁻³	22.2	-	3 months	7.5	31
PVC + nitrobenzene +tetraphenylborate + 2-[(2-hydroxyphenyl) imino]-1,2-diphenylethanone ionophore	1×10 ⁻⁶ – 1×10 ⁻¹	8×10 ⁻⁷	28.5 ±0.5	<20 s	10 weeks	4-11.5	32
calcium ionophore II + ONPE + PVC + potassium tetrakis(p-chlorophenyl)borate	1×10 ⁻⁵ – 1×10 ⁻¹	5.6×10 ⁻⁶	27.2	-	3 months	4-11	33
PVC+ furildioxime + DBP+ potassium tetrakis(p-chlorophenyl)borate	2.6×10 ⁻⁷ –1.0×10 ⁻¹	1.25×10 ⁻⁷	29.5 ±0.5	10 s	3 months	3.5 - 9	34
PVC + KTFPB+ DOS +ETH 100 with the aid of conducting polymer layer of polypyrrole doped with trion	1×10 ⁻⁶ – 1×10 ⁻⁴	1×10 ⁻⁷	28.1	1 min	3 months	7	35
Calcium ionophore (ETH 5234) + (ETH 500) + PVC + o-NPOE.	7.8×10 ⁻⁴ – 7.5×10 ⁻³	-	82.0 ±0.5	-	-	2	36

(ETH 5234) + sodium tetrakis[3,3-bis(trifluoromethyl)phenyl]borate + PVC + o-NPOE	-	-	29.2	-	-	2	36
PVC + KTCIPB + o-NPOE + ETH 1001	$1 \times 10^{-5} - 1 \times 10^{-1}$	1×10^{-6}	25 ± 0.9	-	-	9	37
PVC + KTCIPB + o-NPOE + ETH 1001 with Polymethylthiophene conducting polymer film	$1 \times 10^{-8} - 1 \times 10^{-5}$	-	26.3 ± 0.8	-	-	9	37
The PMT films were modified by 2 days of immersion in an aqueous solution containing 0.1 M EDTA and 0.05 M CaCl ₂	$1 \times 10^{-4} - 1 \times 10^{-1}$	-	30.5 ± 0.4	-	10 days	9	37
dibenzo-18-crown-6 ionophore + PVC + plasticizer	$1 \times 10^{-5} - 1 \times 10^{-1}$	4×10^{-6}	28	< 30 s	5 months	3 - 11	38
Graphite powder + Synthesized ionophore (1,4-diaza-2,3;8,9-dibenzo-7,10-dioxacyclododecane-5,12-Dione) + Acetophenone	$1.3 \times 10^{-6} - 3.2 \times 10^{-3}$	7.9×10^{-9}	32	< 10 s	3 months	3-9	39
Graphite powder + MWCNTs-NiO-Lis composite + paraffin oil + (KTPCIPB)	$1 \times 10^{-2} - 1 \times 10^{-8}$	3.5×10^{-9}	30.43 ± 0.5	10 s	106 days	6- 11	This study

3.6. Analytical application

The studied CPE was applied for the determination of Ca²⁺ ions in tap water, soil drainage water samples, pharmaceutical tablets and human serum. The water samples were collected and stored in polyethylene bottles in darkness at 4 °C before use. The samples were filtered through a 0.45 μm membrane filter and the pH was adjusted to pH 7 with 0.01 mol L⁻¹ hydrochloric acid and 0.1 mol L⁻¹ sodium hydroxide solutions and immediately analyzed. The human serum samples were filtered with 0.22 μm syringe filters before direct measurements. The effectiveness and the reliability of the studied electrode were measured by applying the standard addition experiment on different calcium real samples as being represented in Table 5 and the recovery was ranged from 94.00% to 102.00%. The proposed electrode was successfully applied for the real-time dissolution monitoring of calcium tablets. One tablet of calcium was placed in the dissolution medium and the proposed sensor together with the reference electrode were immersed immediately into the dissolution medium and the potential in mV was recorded every 5 min without the need for frequent sampling at every time interval. The amount of the dissolved calcium was calculated from the attained *e.m.f.* using the equivalent calibration curve and the dissolution profile was plotted. The Osteocare tablet exhibited more than 90% release and reached the plateau from 35 to 45 min as shown in Fig. 8.

Table 5. Determination of Ca²⁺ ion concentration in real samples.

Sample	Determined (mol L ⁻¹)	Added (mol L ⁻¹)	Found (mol L ⁻¹)	Recovery %	RSD %
Osteocare tablets	-	-	1.0×10^{-4}	-	-
	1.01×10^{-4}	5×10^{-4}	6.0×10^{-4}	99.8	1.09
	1.0×10^{-4}	10×10^{-4}	10.8×10^{-4}	98.0	0.97
	1.02×10^{-4}	15×10^{-4}	16.1×10^{-4}	100.5	1.12
Tap water	-	-	1.5×10^{-3}	-	-
	1.5×10^{-3}	5×10^{-3}	6.2×10^{-3}	94.0	1.23
	1.5×10^{-3}	10×10^{-3}	11.7×10^{-3}	102.0	1.17
	1.5×10^{-3}	15×10^{-3}	16.1×10^{-3}	97.3	1.35
	-	-	2.05×10^{-4}	-	-

Soil drainage water	2.0×10^{-4}	5×10^{-4}	6.7×10^{-4}	94.0	1.54
	2.0×10^{-4}	10×10^{-4}	11.6×10^{-4}	96.0	1.58
	2.1×10^{-4}	15×10^{-4}	16.5×10^{-4}	96.0	1.72
Serum ionic Calcium	-	-	1.2×10^{-3}	-	-
	1.2×10^{-3}	1×10^{-3}	2.18×10^{-3}	98.0	2.13
	1.2×10^{-3}	5×10^{-3}	6×10^{-3}	96.0	2.54
	1.3×10^{-3}	7×10^{-3}	8.2×10^{-3}	98.6	2.17
	1.3×10^{-3}	1×10^{-5}	13.09×10^{-4}	95.1	2.26
	1.3×10^{-3}	1×10^{-4}	13.97×10^{-4}	97.0	1.98

The validity of the proposed CPE for calcium ion determination in standard solutions and human serum was examined through the comparison of its results with those of the HPLC-ELSD reported method [24] and Spectrophotometric complexation with murexide reported method [46], respectively, using the student's t-test and variance ratio F-test at $p = 0.05$. Table 6 shows that the calculated t- and F-values were lower than the theoretical values. It indicates no significant difference between the mean and variances of both methods in the determination of Ca^{2+} ions.

Table 6. Statistical comparison between the proposed CPE and the reported HPLC-ELSD and Spectrophotometric methods for the determination of Ca^{2+} ions.

Parameter	Ca^{2+} standard solution		Serum ionic Ca^{2+}	
	CPE	Published method ¹	CPE	Published method ³
Mean	99.56	99.86	96.94	97.67
SD	1.13	1.04	1.42	1.87
Variance	1.28	1.08	2.02	3.50
N	5	5	5	5
Student's t-test (2.31) ²	0.44		0.7	
F-test (6.39) ²	0.84		1.73	

¹The published method was based on using HPLC using ELSD with nitrogen gas flow rate of ELSD 2.5 L/min [24].

²The figures in parenthesis are the theoretical values of t and F at $p = 0.05$.

³The published method for serum ionic calcium was based on the spectrophotometric determination of Ca^{2+} after the formation of a colored complex with murexide that was measured at 470 nm [46].

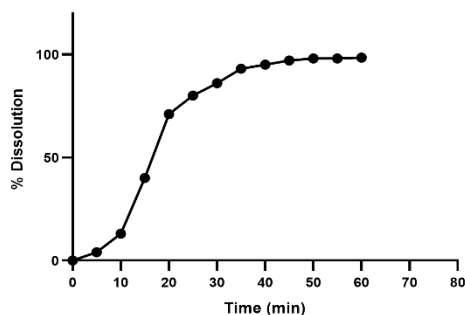


Figure 8. The dissolution profile of calcium Osteocare tablets using the proposed CPE.

4. CONCLUSION

In conclusion, for the first time, lisinopril was covalently grafted on MWCNTs-NiO nanocomposite. The resulting material was applied as a novel electroactive nanomaterial in the fabrication of Ca²⁺ selective potentiometric CPE. It was characterized by FT-IR, XRD, and TEM that confirmed the covalent functionalization of the lisinopril molecules to the MWCNTs-NiO nanocomposite surface. The proposed sensor exhibited good selectivity and sensitivity to Ca²⁺ ions. It exhibits a linear response over a wide concentration range from 1×10⁻² mol L⁻¹ to 1×10⁻⁸ mol L⁻¹ with a Nernstian slope of 30.4 ±0.52 mV/decade over the pH range from 6 to 11. The CPE was successfully applied for the determination of Ca²⁺ ions in tap water, soil drainage water samples, human serum samples and pharmaceutical tablets without any prior extraction processes. It was efficiently used in monitoring the dissolution profile of calcium tablets. The proposed CPE can be efficiently applied for the quantitation of Ca²⁺ ions in routine control work.

CONFLICT OF INTEREST

No potential conflict of interest relevant to this article was reported.

References

1. K.L. Goa, M. Haria and M.I. Wilde, *Drugs*, 53 (1997) 1081.
2. A.A. El-Habeeb, *Res. J. Pharm. Biol. Chem. Sci.*, 6 (2015) 2034.
3. S.L. Wang, C.H. Chuang and S.Y. Lin, *Chem. Pharm. Bull.*, 50 (2002) 78.
4. M. Zaky, M.Y. El-Sayed, S.M. El-Megharbel, S.A. Taleb and M.S. Refat, *J. Mex. Chem. Soc.*, 58 (2014) 142.
5. M. Remko, *Chem. Pap.*, 61 (2007) 133.
6. V.K. Thakur and M.K. Thakur, *Chemical Functionalization of Carbon Nanomaterials Chemistry and Applications*, CRC Press Taylor & Francis Group (2016) Boca Raton, Florida.
7. N.A. Abdallah, *Sensors and Materials*, 28 (2016) 797.
8. N.A. Abdallah, *J. Electrochem. Soc.*, 167 (2020) 047504.
9. N.A. Abdallah and S. Ahmed, *J. Electrochem. Soc.*, 165 (2018) H756.
10. N.A. Abdallah and H.F. Ibrahim, *Carbon Letters*, 27 (2018) 50.
11. N.A. Abdallah, *Int. J. Electrochem. Sci.*, 11 (2016) 10715.
12. M. Baro, P. Nayak, T.T. Baby and S. Ramaprabhu, *J. Mater. Chem. A*, 1 (2013) 482.
13. X. Luo, A. Morrin, A.J. Killard and M.R. Smyth, *Electroanalysis*, 18 (2006) 319.
14. H.W. Gao, *J. Braz. Chem. Soc.*, 13 (2002) 78.
15. L.A. Jamil and S.A. Rahim, *IOP Conf. Ser. Mater. Sci. Eng.*, 454 (2018) 012089.
16. L. Zaijun, T. Jian and P. Jiaomai, *Anal. Chim. Acta*, 452 (2002) 303.
17. R.R. Gangidi and L.E. Metzger, *J. Dairy Sci.*, 89 (2006) 4105.
18. Y. Hua, Q. Wei, G. Wu, Z.B. Sun and Y.J. Shang, *Anal. Lett.*, 53 (2019) 960.
19. L. Lu, X. An and W. Huang, *Anal. Methods*, 9 (2017) 23.
20. S. Mahgoub, *Ann. Chromatogr. Sep. Tech.*, 3 (2017) 1028.
21. M. Meléndez, E.P. Nesterenko, P.N. Nesterenko and J.E. Corredor, *Limnol. Oceanogr.: Methods*, 11 (2013) 466.
22. S. Rahimi-Yazdi, M.A. Ferrer and M. Corredig, *J. Dairy Sci.*, 93 (2010) 1788.
23. M. Song, J. Park, J. Lee, H. Suh, H. Lee, D. Ryu and C. Lee, *Foods*, 9 (2020) 248.
24. Q. Tang, X. Wang, F. Chen and X. Tan, *J. Pharm. Biomed. Anal.*, 77 (2013) 29.

25. B. Deng, P. Zhu, Y. Wang, J. Feng, X. Li, X. Xu, H. Lu and Q. Xu, *Anal. Chem.*, 80 (2008) 5721.
26. M.A.T. Lemos, A.M. Pinheiro, R.J. Cassella and D.P. Jesus, *Anal. Methods*, 6 (2014) 3629.
27. M. Patsar-Kallio and P.K.G. Manninen, *Anal. Chim. Acta*, 314 (1995) 67.
28. J.M.S. Almeida, R.M. Dornellas, S. Yotsumoto-Neto, M. Ghisi, J.G.C. Furtado, E.P. Marques, R.Q. Aucélio and A.L.B. Marques, *Fuel*, 115 (2014) 658.
29. D.G. Dilgin, *Anal. Lett.*, 51 (2017) 186.
30. B. Kabagambe, M.B. Garada, R. Ishimatsu and S. Amemiya, *Anal. Chem.*, 86 (2014) 7939.
31. J. Saurina, E. López-Aviles, A.L. Moal and S. Hernández-Cassou, *Anal. Chim. Acta*, 464 (2002) 89.
32. M.R. Ganjali, H.A. Zamani, M. Adib and M. Accedy, *Acta Chim. Slov.*, 52 (2005) 309.
33. K.Y. Chumbimuni-Torres and L.T. Kubota, *J. Food Compost. Anal.*, 19 (2006) 225.
34. A.K. Singh and S. Mehtab, *Sens. Actuators B Chem.*, 123 (2007) 429.
35. A. Konopka, T. Sokalski, A. Michalska, A. Lewenstam and M. Maj-Zurawska, *Anal. Chem.*, 76 (2004) 6410.
36. S. Liu, J. Ding and W. Qin, *Anal. Chim. Acta*, 1031 (2018) 67.
37. A. Michalska, A. Konopka and M. Maj-Zurawska, *Anal. Chem.*, 75 (2003) 141.
38. A. Kumar and S.K. Mittal, *Sens. Actuators B Chem.*, 99 (2004) 340.
39. M. Shamsipur, G. Khayatian, S.Y. Kazemi, K. Niknam and H. Sharghi, *J. Incl. Phenom. Macrocycl. Chem.*, 40 (2001) 303.
40. S.S. Hossain, J. Saleem, A.A. Ahmed, M.M. Hossain, M.N. Shaikh, S.U. Rahman and G.M. Kay, *Int. J. Electrochem. Sci.*, 11 (2016) 2686.
41. P. Junlabhut, C. Bangbai and C. Kahattha, *Thai J. Nanosci. Nanotechnol.*, 1 (2016) 17.
42. J. Safari and S. Gandomi-Ravandi, *J. Iran. Chem. Soc.*, 12 (2014) 147.
43. E.B. Gonzalez, E. Farkas, A.A. Soudi, T. Tan, A.I. Yanovsky and K.B. Nolan, *J. Chem. Soc., Dalton Trans.*, 13 (1997) 2377.
44. T. Jurca, E. Marian, L.G. Vicaş, M.E. Mureşan and L. Fritea, *Metal Complexes of Pharmaceutical Substances*, in: *Spectroscopic Analyses - Developments and Applications*, Intechopen (2017).
45. Y. Umezawa, P. Buhlmann, K. Umezawa, K. Tohda and S. Amemiya, *Pure Appl. Chem.*, 72 (2000) 1851.
46. A. Raman, *Clin. Biochem.*, 5 (1972) 208
47. N.A. Abdallah and H.F. Ibrahim, *Microchem. J.*, 147 (2019) 487.
48. N.A. Abdallah, *Electroanalysis*, 33 (2021) 1283